Available online at www.sciencedirect.com
SCIENCE DIRECT®
Journal of Power Sources 145 (2005) 534–545
JOURNAL OF POWER SOURCES
www.elsevier.com/locate/jpowsour

Polymer electrolyte fuel cell stack thermal model to evaluate sub-freezing startup

M. Sundaresan [a,*], R.M. Moore [b]

[a] *University of California, One Shields Avenue, Davis, CA 95616, USA*
[b] *University of Hawaii, USA*

Accepted 30 December 2004
Available online 26 April 2005

Abstract

For passenger fuel cell vehicles (FCVs), customers will expect to start the vehicle and drive almost immediately, implying a very short system warmup to full power. While hybridization strategies may fulfill this expectation, the extent of hybridization will be dictated by the time required for the fuel cell system to reach normal operating temperatures. Quick-starting fuel cell systems are impeded by two problems: (1) the freezing of residual water or water generated by starting the stack at below freezing temperatures and (2) temperature-dependent fuel cell performance, improving as the temperature reaches the normal range. Cold start models exist in the literature; however, there does not appear to be a model that fully captures the thermal characteristics of the stack during sub-freezing startup conditions. Existing models lack the following features: (1) modeling of stack internal heating methods (other than stack reactions) and their impact on the stack temperature distribution and (2) modeling of endplate thermal mass effect on end cells and its impact on the stack temperature distribution.

The focus of this research is the development and use of a sub-freezing thermal model for a polymer electrolyte fuel cell stack. Specifically, the work has focused on the generation of a model in which the fuel cell is separated into layers to determine an accurate temperature distribution within the stack. Unlike a lumped model, which may use a single temperature as an indicator of the stack's thermal condition, a layered model can reveal the effect of the endplate thermal mass on the end cells, and accommodate the evaluation of internal heating methods that may mitigate this effect.

Keywords: Polymer electrolyte fuel cell; Cold start; Thermal model; Temperature distribution

1. Introduction and problem statement

In early 2002, the U.S. Department of Energy (DOE) announced a new partnership with USCAR (consortium of Big Three automakers DaimlerChrysler, Ford and General Motors) called FreedomCAR whose goal is to reduce U.S. dependence on petroleum through the development of hydrogen-powered fuel cell cars and light trucks. The primary focus of FreedomCAR is on basic research to provide fuel cell vehicles that use no petroleum. Considerable research and development effort has been funded through DOE under FreedomCAR's predecessor, the Partnership for a New Generation of Vehicles (PNGV), for hydrogen/air fuel cells powered directly by hydrogen and indirectly with other fuels. While much progress has been made on advancing fuel cell systems, the primary challenges for direct hydrogen systems are the lack of retail refueling infrastructure, on-board hydrogen storage, cost, durability, size and weight [1].

In addition to these challenges, reducing system startup time can produce interesting implications for the system configuration, such as the need to hybridize, which adds complexity and possibly cost. For passenger fuel cell vehicles, customers will expect to start the vehicle and drive almost immediately, implying a very short system warmup to full power. For the direct hydrogen system, the current DOE requirement for the 2010 goal of cold startup from −20 °C to maximum power is 30 s [2]. While there is debate on the con-

* Corresponding author. Tel.: +1 530 792 1033.
E-mail address: meena.sundaresan@sbcglobal.net (M. Sundaresan).

0378-7753/$ – see front matter © 2005 Elsevier B.V. All rights reserved.
doi:10.1016/j.jpowsour.2004.12.070

Nomenclature

c_p	specific heat ($J\,kg^{-1}\,K^{-1}$)
m	mass (kg)
P	power (W)
t	time (s)
T	temperature (K)

ditions in which hybridization would be useful, given complexity and added cost [3], some studies concede that the cold start operation would require hybridization [4–7].

While hybridization strategies may fulfill the expectation of rapid driveaway, the extent of hybridization will be dictated by: (1) the time required for the fuel cell system to reach normal operating temperatures, (2) packaging limits in real vehicles, and (3) effects of added weight. The results of an analysis tool to explore methods to minimize the startup time are described in this paper.

1.1. Problem statement

A cold start fuel cell stack thermal model is a tool that can be used to analyze different warming strategies. However, a model that fully captures the thermal characteristics of the stack during sub-freezing cold start is not currently available. Based on an evaluation of existing cold start stack thermal models in the literature [8], a new cold start stack thermal model is necessary to meet the criteria defined for an acceptable cold start simulation.

Existing models lack the following features:

- Modeling of stack internal heating methods (other than stack reactions) and their impact on the stack temperature distribution.
- Modeling of endplate thermal mass effect on end cells and its impact on the stack temperature distribution.

Existing cold start stack thermal models address and model external heating methods as well as heat generated internally due to stack reactions. However, these models consider the stack as a lumped mass and do not also accommodate the evaluation of other internal heating methods that are more easily included when the individual cell layers are modeled. Part of the evaluation of these heating methods includes observing the stack temperature distribution and even the cell temperature distribution to investigate temperature excursions within sensitive components such as the polymer electrolyte membrane (PEM). (PEM fuel cell stacks are considered suitable for transportation applications because they provide continuous electrical energy at high efficiency and power density [9]).

Furthermore, these models do not explicitly account for the effect of the endplate thermal mass on the stack. The thermal mass of the endplates draws heat from the cells at both ends of the stack and affects the stack temperature distribution. Existing models use a single stack temperature or stack coolant outlet temperature, for example, as an indicator of the stack's thermal condition; however, in a model in which the cell layers are separate, the condition of each cell within the stack can be observed. For example, if the stack cannot operate until it is heated to 0 °C, a single temperature may hide the fact that the end cells are lower than 0 °C, resulting in ice formation if the stack is operated.

The new, one-dimensional, layered cell thermal model was developed using Matlab®/Simulink® software and considers the features, in addition to those found in existing models, which form an analysis tool for sub-freezing cold start of a PEM fuel cell stack. The model includes those features not considered by existing cold start stack thermal models, namely the ability to observe the impact on the stack temperature distribution by stack internal heating methods (including, but not limited to, stack reactions) and the endplate thermal mass effect on end cells. In a transportation application, such as a direct hydrogen hybrid fuel cell vehicle, the cold start operation generally includes the entire fuel cell system. Therefore, the layered cell thermal model is incorporated into a fuel cell system in which system component thermal masses have also been included. The cold start thermal model simulates startup for a non-moving vehicle. It is understood that the cooling loop heat fluxes may be different while the vehicle is being driven. However, these interactions are not within the scope of this paper.

The simulations are performed with literature-based parameter values that do not necessarily represent the state-of-the-art. The purpose of the model is not to show how to attain the DOE goal of 30 s from −20 °C to "maximum power" [2], for example, but to demonstrate the benefits of this model as a tool for cold start analysis.

1.2. Organization of paper

This paper is organized in two major sections: (1) model description and (2) simulation results that highlight the capabilities of the layered cell thermal model and compare methods to reduce startup time.

2. Model generation

2.1. System

The cold start operation generally includes the entire fuel cell system cooling loop, for which the components are typically a stack, compressor and humidifier for a direct hydrogen system. Vehicle components such as the coolant pump are included, as well as the radiator fan motor, traction motor and radiator when they are not bypassed. The cooling loop serves to carry heat from an external heat source to the stack and system components or circulate stack internal heat. A general schematic of the coolant loop is shown in Fig. 1. Note that the simulation results presented in this paper do not include

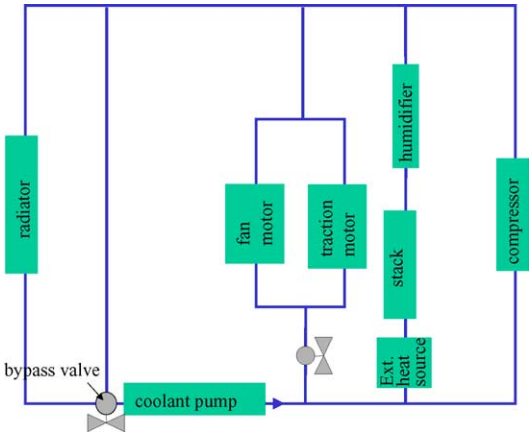

Fig. 1. Cooling loop schematic.

the use of the external heat source but only account for its thermal mass; the results for simulations using an operating external heat source are presented elsewhere [8].

One coolant loop configuration is considered in the simulation results presented in this paper: a small loop, including the pump, stack, non-operating external heat source, and coolant for these components plus coolant in the stack manifold and piping, as shown in Fig. 2.

The small loop (with non-operating external heat source but with internally heated stack) is used as the simulation baseline configuration because it is the least thermally massive configuration that accommodates circulation. The model accommodates the comparison of scenarios with the coolant circulation on and off to show the effect of both conditions on the stack's temperature distribution during warmup. Simulation results with the addition of system and vehicle thermal masses are presented elsewhere [8].

2.2. Stack

The stack is characterized on a cell basis, i.e. a layered cell thermal model is developed using first principles, duplicated and included with endplates to represent a stack.

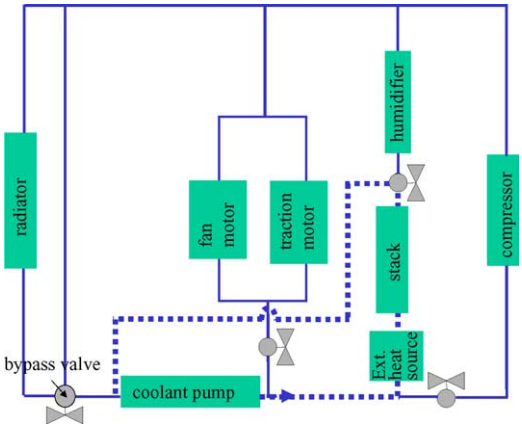

Fig. 2. Small loop configuration.

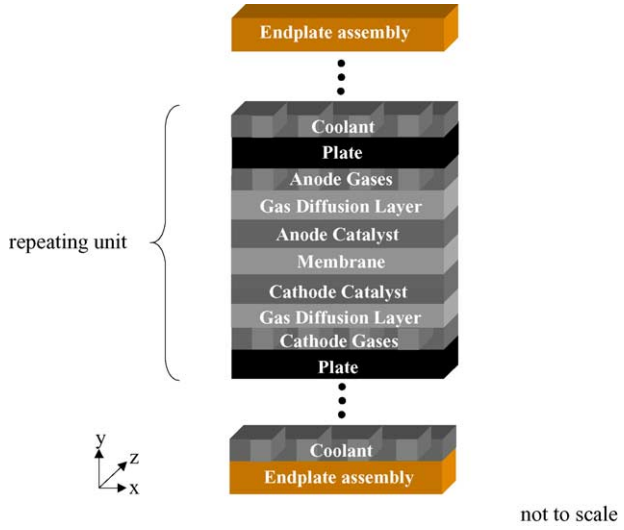

Fig. 3. Overview sketch of cell unit and endplates.

The model is built using energy and mass balances at each layer including sensible energy flows for coolant and anode and cathode gases. Water generation and phase changes (vapor, liquid and ice in the case of sub-freezing temperatures), stack heat losses to the environment, as well as internal heat generation by the electrochemical reactions and ohmic resistance are considered. The primary result of the calculations is the layer midpoint temperature as a function of time. Heat generation is not limited to stack reactions. Other heating methods as well as water management strategies considered on a cell/stack level in the model are those proposed in the literature [8].

The layers in the cold start cell thermal model include bipolar plates (with cooling and gas channels), gas diffusion layer (GDL), catalyst support, and membrane, and a complete stack includes an endplate assembly (end plate, bus plate, and interface (I/F) plate) (see Fig. 3). The cell model is one-dimensional (along the *y*-axis) in which the temperature at the center of each layer is calculated (see Fig. 4). For a detailed description of the cell model and a listing of all the equations, assumptions and parameters used, refer to [8]. All cells in the stack are built with the same 10 layers (i.e. the middle section in Fig. 3 is a repeating unit). While every cell of a full stack of (an arbitrarily selected) 225 cells could be modeled, for computational efficiency it was determined that a minimum of 30 cells plus an extra cooling layer for symmetry and two endplate assemblies could represent a full stack [8]. Energy and mass balances are maintained within the model. Validation of the model is detailed in [8].

3. Simulation results and discussion

The results of simulations performed with the layered cell cold start thermal model are detailed in this section. The results highlight the capabilities of a layered model when com-

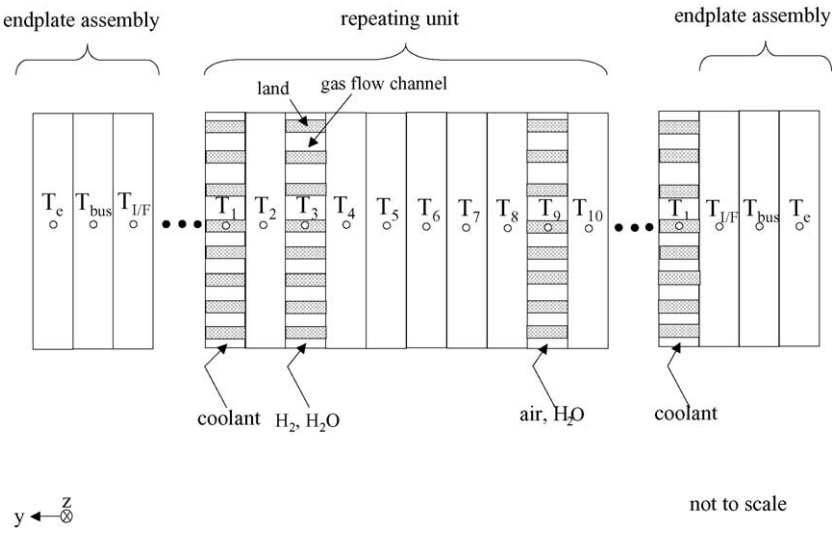

Fig. 4. Model sketch of cell unit and endplates.

pared to a lumped analysis, and show the value of a layered model, especially for the cells by the endplates. The layered model is then used as a cold start model to evaluate various startup scenarios including, but not limited to, those considered by existing cold start models described in the literature.

The simulation boundary conditions are explained as follows. The conditions selected represent two distinct periods of interest: (1) sub-freezing ambient temperature (T_{amb}) to stack operating temperature ($T_{threshold}$), and (2) stack operating temperature ($T_{threshold}$) to *vehicle propulsion* stack operating temperature ($T_{setpoint}$). Condition 1 starts from T_{amb} and ends at $T_{threshold}$, and Condition 2 starts at $T_{threshold}$ and ends at $T_{setpoint}$.

These conditions are met using one of the following two temperatures as a trigger: (1) a single stack temperature, a practical but incomplete metric to assess the stack's thermal condition, and (2) the cathode catalyst layer temperature. Some comparisons are made using the cathode catalyst layer temperature of the *middle* cell and of the *coldest* cell to distinguish the two when considering that fuel cell operation at $T_{threshold}$ below 0 °C, for example, can result in ice formation from product water at the cathode catalyst. In the investigations shown in the following sections, these temperatures are compared in terms of the useful information provided by them for control purposes.

The simulation results are divided into four parts:

- Section 3.1 shows a preliminary lumped analysis performed to establish a reference against which the layered model results can be compared.
- Section 3.2 investigates the stack thermal condition with the layered model showing how some cell layers or entire cells can be colder than expected as compared to a single lumped parameter temperature of 0 °C. The simulations are performed with the stack off and warmed until the selected trigger reaches $T_{threshold}$ of 0 °C to determine if cell layers, especially cathode catalyst layers, are still below 0 °C and could generate ice if the stack was subsequently operated.
- Section 3.3 investigates the stack thermal condition in an extreme case with the layered model showing how some cell layers or entire cells can be hotter than expected as compared to a single lumped parameter temperature of 80 °C. The simulations are performed with the stack off and warmed until the selected trigger reaches $T_{threshold}$ of 80 °C to determine if cells exceed 80 °C and by what magnitude.
- The benefits of a layered model, highlighted in Sections 3.2 and 3.3, are exploited in Section 3.4 as the layered model performs its intended function—as a cold start model used to evaluate various heating methods and to evaluate the effect of ice formation and melting.

Sections 3.2–3.4 begin with a description of the simulation conditions and parameter (and parameter variation, if applicable) lists, followed by results and discussion.

3.1. Preliminary lumped analysis

Lumped parameter stack cold start analysis represents the literature state-of-the-art. The purpose of the preliminary lumped analysis here is to obtain a reference for the layered stack model used in this paper.

Based on the parameters shown in Table 1, a lumped analysis using Eq. (1) is performed to determine energy consumption and time required for the thermal mass to reach a desired

Table 1
Summary of stack and small loop thermal mass

Component	Mass × specific heat, mc_p (J K^{-1}) [8]
Stack + coolant	89494
Small loop	14690
Total	104184

temperature.

$$\Delta E = mc_p\Delta T, \qquad \Delta E = P\Delta t \tag{1}$$

This analysis is divided into two parts: a *stack lumped case* and *system lumped case*, which includes the thermal mass of components in a small cooling loop. *Stack lumped case* is defined by the following points:

(1) No effect on end cells (since there are no "end cells") due to the endplate thermal mass, although the endplate thermal mass itself is taken into account.
(2) No losses to the environment. These losses are insignificant (∼1%) relative to the heat draw of the endplate thermal mass determined by the layered model in this paper. Other studies neglect these losses altogether [10,11].
(3) Temperature range is −20 to 0 °C. The upper temperature limit of 0 °C was selected for the lumped analysis to compare with the layered model for which several results are based on simulations with an upper limit of 0 °C.
(4) The thermal mass of the stack/endplates and stack and manifold coolant are considered. Note that the thermal mass calculations for the coolant use one value for the coolant specific heat unlike the layered model, which uses a curve fit of the temperature-dependent specific heat (see [8]).

System lumped case includes the above conditions in the *stack lumped case*, plus the additional thermal mass (as noted in Table 1).

3.1.1. Stack lumped case

Using the thermal mass for the stack/endplates, stack coolant and manifold coolant found in Table 1, one can calculate the energy and time required by an 11 250 W heat source (power level selected to match level used for internal heating in the model, i.e. 50 W × 225 cells) until $T_{\text{threshold}}$.

$$\Delta E = mc_p\Delta T,$$

$$1\,789\,880\,\text{J} = 89\,494\,\text{J K}^{-1} \times (273 - 253)\,K,$$

$$\Delta t = 1\,789\,880\,\text{J}/11\,250\,\text{J s}^{-1} \approx 159\,\text{s}$$

3.1.2. System lumped case

A similar calculation can be performed for the system lumped case, considering components in a small cooling loop. Using an 11 250 W heat source (power level selected to match level used for internal heating in the model) until $T_{\text{threshold}}$ results in the following time.

$$\text{small loop}: \quad 2\,083\,680\,\text{J} = 104\,184\,\text{J K}^{-1} \times (273 - 253)\,K,$$

$$\Delta t = 2\,083\,680\,\text{J}/11\,250\,\text{J s}^{-1} \approx 185\,\text{s}$$

The energy and time calculated in the stack and system lumped cases are compared with layered model results shown in the next section.

3.2. Stack operation at 0 °C, layered model

3.2.1. Simulation conditions and description

This section investigates the issue of starting the stack at 0 °C when some cells are actually below 0 °C, risking ice formation. A comparison is made between the single stack temperature used in the lumped analysis and the *middle* cell cathode catalyst layer temperature used in the layered model. Using Condition 1 of the boundary condition definitions described earlier, the layered model simulation runs with T_{amb} of −20 °C until the trigger reaches $T_{\text{threshold}}$ of 0 °C by internal heating. The initial temperature, T_{amb}, was selected as −20 °C to match the DOE requirements for 2010 [2]. The stack operating temperature, $T_{\text{threshold}}$, is set at 0 °C, but the stack in fact never turns on during these simulations. The purpose is to show how the stack may be colder than expected depending on the temperature used to determine stack readiness for operation. The layered model temperature distribution shows that by selecting the *middle* cell cathode catalyst layer temperature as the trigger, the end cells can still be below 0 °C.

Then simulation results using the *coldest* cell cathode catalyst layer as the trigger show the additional time and energy required to bring this layer to 0 °C. Further results illustrate the effect of independently varying parameters (e.g. bipolar plate material, endplate mass and condition, heat input level, and coolant flow) on the additional time and energy required. A summary of the parameters is shown in Table 2 and the variation on the parameters is shown in Table 3.

3.2.2. Results and discussion

The results in this section are based on the parameters found in Tables 2 and 3. The single stack temperature used in the lumped analysis and the layered model's middle and coldest cell cathode catalyst layer temperatures, when used as the triggers, are compared in Fig. 5. Recall the discussion in Section 2.2 of the model construction: there are 30 cells with endplate assemblies modeled. Therefore, for the temperature distribution plots shown in this section, 307 points are plotted,

Table 2
Parameter summary, 0 °C case

Parameter	Value
T_{amb}	−20 °C
$T_{\text{threshold}}$	0 °C
Trigger temperature	Middle cell cathode catalyst layer temperature vs. coldest cell cathode catalyst layer temperature (used as baseline for variation runs)
Heat source	50 W in each cell membrane, e.g. power from electric wire [8]
Cell bipolar plate material (cell layers 1–3, 9 and 10)	Graphite
Endplate mass	As indicated in [8]
Endplate condition	Unheated
Coolant flow	Off vs. on (used as baseline for variation runs)

Table 3
Parameter variation, 0 °C case

Parameter	Baseline	Variation
Heat source	50 W per cell (in membrane, e.g. electric wire [8])	100 W per cell
Cell bipolar plate material (cell layers 1–3, 9 and 10)	Graphite	Stainless steel (316L)[a]
Endplate mass	As indicated in [8]	50% less
Endplate condition	Unheated	Heated with power required to "flatten" temperature distribution (175 W each)

[a] Thickness, $t = 0.1$ mm source: [12], thermal conductivity, $k = 13.4$ W m^{-1} K^{-1}, density = 8238 kg m^{-3}, specific heat, $c_p = 468$ J kg^{-1} K^{-1}, specific resistance = 7.4×10^{-7} Ω m.

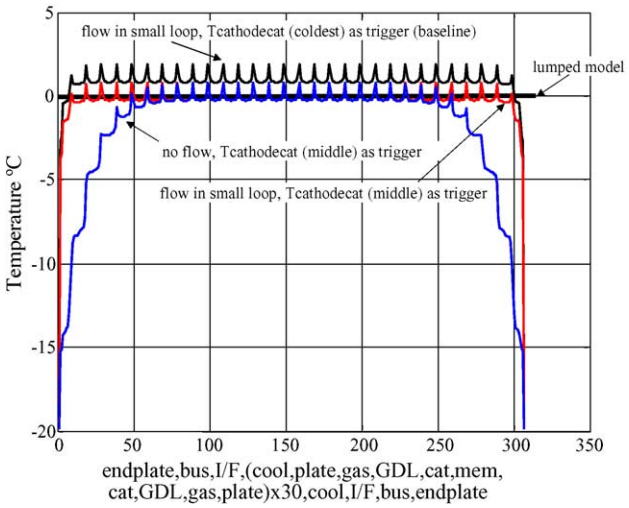

Fig. 5. Stack temperature distribution, trigger comparison.

i.e. 30 cells with 10 layers each plus an extra cooling layer for symmetry and six layers representing the endplate assemblies for each end of the stack.

Note the differences between the three cases shown in Fig. 5. When there is coolant flow, heat from the middle cells is distributed to the end cells which are affected by the heat draw of the endplates. It is assumed that the coolant pump output may be low in a sub-freezing condition and higher, but controlled by stack temperature, during normal operation.

The effect of the endplate thermal mass is more pronounced in the no-flow condition. In both cases in which the middle cell cathode catalyst layer temperature is the trigger, there are end cell temperatures below 0 °C. Keeping the flow on to maintain a more homogeneous temperature distribution, the trigger is changed to the coldest cell cathode catalyst layer temperature, ensuring that all cells are at or above 0 °C. These conditions are used to establish a baseline for the next set of results.

For the baseline layered model, simulations are performed independently varying heat output, bipolar plate material, endplate mass, endplate condition (unheated or heated), and coolant flow (on or off). Fig. 6 compares time and energy for the lumped analysis and layered model, the trigger com-

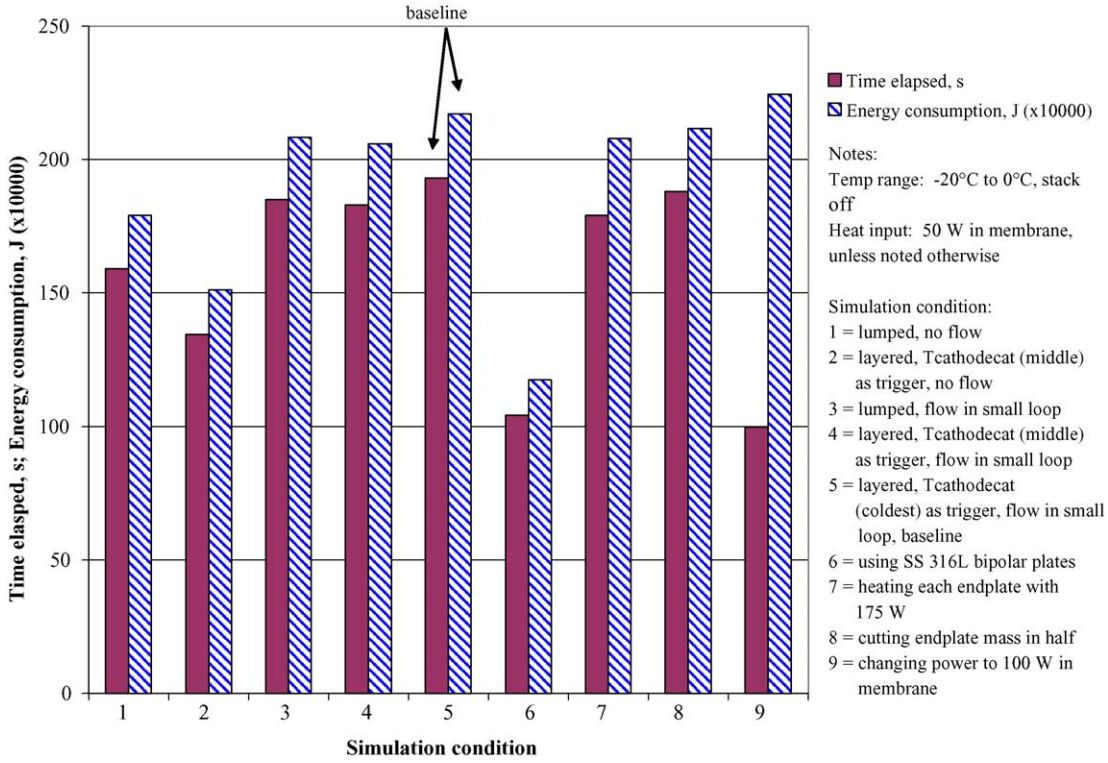

Fig. 6. Time elapsed and energy consumed vs. simulation condition, 0 °C case.

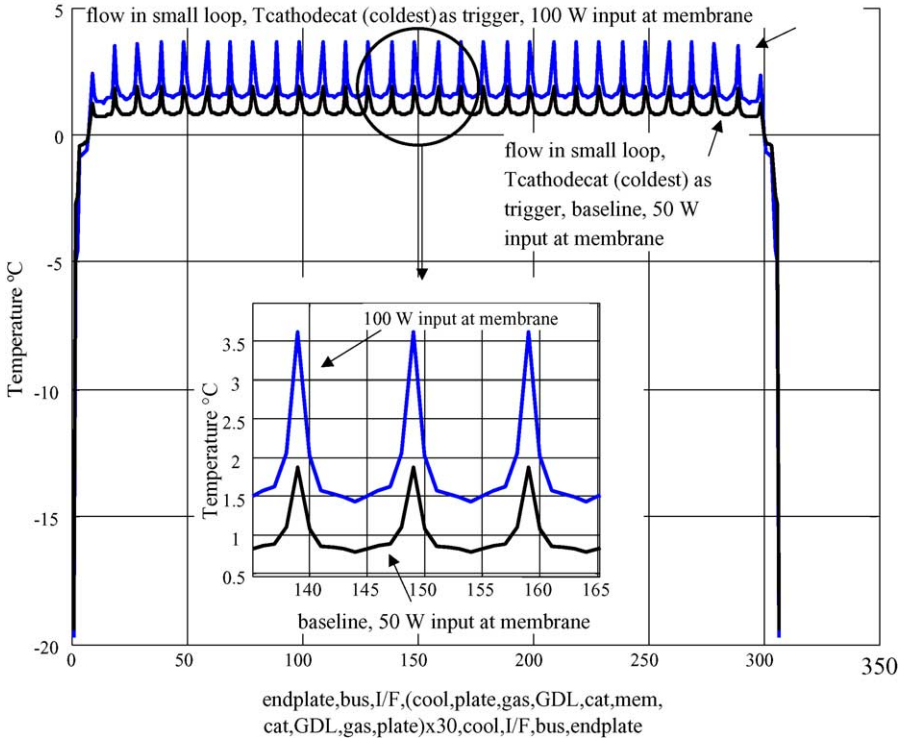

Fig. 7. Stack temperature distribution, 100 W.

parison, as well as the parameter variations against the baseline.

In Fig. 6, the case with the layered model, no flow, and middle cell cathode catalyst layer as the trigger (bar 2) shows a time less than the 159 s previously determined in the lumped analysis (value from Section 3.1 shown in bar 1). The reason for this discrepancy lies in the coolant circulation. For the no-flow case, the middle cell cathode catalyst layer heated to $T_{\text{threshold}}$ quickly, while the end cells lagged, as shown in Fig. 5.

In Fig. 6, the case with flow in a small loop and middle cell cathode catalyst layer as the trigger (bar 4) shows a time slightly less than the 185 s found in the lumped analysis for the small loop (shown in bar 3) because the coolant circulation imparts heat to the end cells raising their temperatures much nearer to 0 °C. This case shows that the lumped and layered models are actually similar in their times, indicating that the lumped model could be a sufficient tool under certain conditions. However, the lumped model lacks the information required to characterize the end cells for which a temperature gradient still exists.

Finally, the scenario in which the layered model uses the coldest cathode catalyst as the trigger (bar 5 and baseline for future simulations) shows an increase from the lumped analysis in time and energy, due to the continued heating up of the other cells in waiting for the coldest cell to reach $T_{\text{threshold}}$.

Some observations can be made about Fig. 6 compared to the baseline (bar 5), such as: (1) around the same energy is consumed for 100 W applied in the membrane in around half the time (bar 9) and the temperature rise in the membrane approximately doubled (see Fig. 7), (2) there is a 46% reduction in time and energy for stainless steel bipolar plates (bar 6) due to a reduction in thickness and thermal mass, and (3) there is a 3% reduction in time and energy for cutting the endplate mass in half (bar 8).

It was found that using 175 W at each endplate (specifically, power applied to the copper bus layer of the endplate assembly) had the effect of bringing the end cells, especially the coldest cell, up to temperature faster, reducing the time by 7% and energy required by 4% (shown in bar 7 in Fig. 6). The temperature distribution in Fig. 8 illustrates the effect of heating the endplates on the end cells.

An application of heating the endplates can be in maintaining above-freezing conditions for the stack. A comparison in energy consumption can be made to a scenario in which the stack is not allowed to drop below 0 °C, for example, by reducing the temperature at shutdown to just above 0 °C and introducing an electrical heat input (requiring on- or off-board power). It was found in the model that a 0.05 W per cell internal heat input and 10 W at each endplate bus layer could maintain the coldest cell above 0 °C, assuming four sides of the stack are perfectly insulated and the heat loss to ambient is through the effectively insulated endplates. Keeping the coolant off eliminates the need for pump power; however, if electrical power is used anyway for heating, it can be used for the pump.

Considering a 12 h period of inoperation, for example, the total energy required would be 1 350 000 J, which is 0.375 kWh of electric source energy. The total energy re-

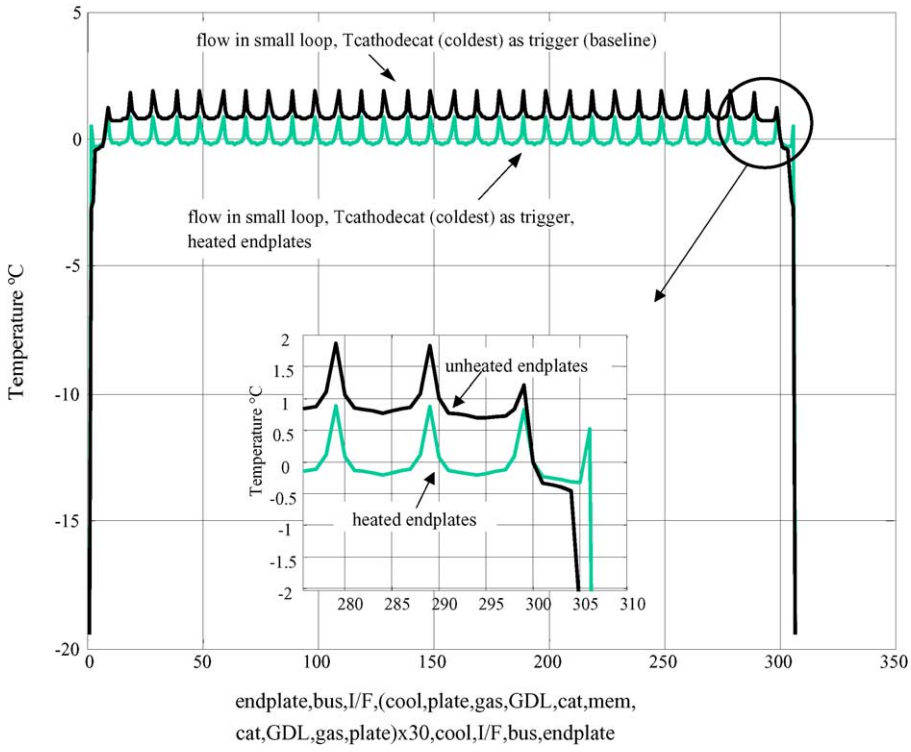

Fig. 8. Stack temperature distribution, heated endplates.

quired would be less than the amounts shown in most of the scenarios in Fig. 6, given the startup conditions and stack thermal characteristics. Of course, this analysis depends on the length of the inoperation period and may not be suitable, for example, for long-term vehicle parking. Fig. 9 shows the temperature distribution for the 0.05 W per cell internal heat input and 10 W at each endplate bus layer for both coolant circulation conditions. Note that the ambient temperature is −20 °C; therefore, the polymer endplate layer (the outermost layer of the endplate assembly) is below 0 °C but has been heated to above −20 °C.

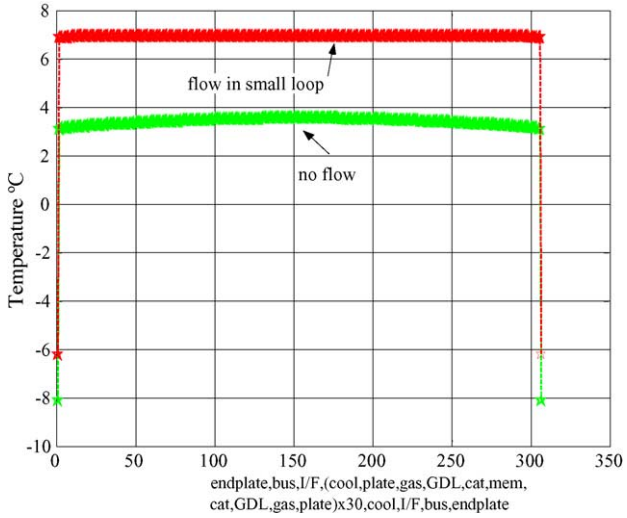

Fig. 9. Stack temperature distribution, heated endplates, kept above 0 °C.

This section has illustrated the detailed information a layered model provides when considering a $T_{threshold}$ of 0 °C. The next section investigates the effect of an extreme case, such as an unusually high heat input within the cell, this time considering a $T_{threshold}$ of 80 °C.

3.3. Extreme case, layered model

3.3.1. Simulation conditions and description

This section investigates an extreme case of a 500 W per cell internal heat input using the layered model. Such a heat input could be, for example, a result of temperature excursions or hot spots from chemical reactions (between H_2 and O_2, used as a heating method) carried out on either or both electrodes [8]. A 500 W internal input would obviously warm the stack within a shorter period of time than 50 W; however, the layered model illustrates the effect of such a heat input on each cell's internal temperature distribution. This case considers a temperature range from T_{amb} of −20 °C to the stack operating temperature $T_{threshold}$ of 80 °C reached by the selected temperature trigger.

As in the previous section, the stack never turns on during these particular simulations. A comparison is made between (1) a single stack temperature of 80 °C and (2) the triggers of the middle and coldest cell cathode catalyst layer temperatures reaching 80 °C. In this case, using the coldest cell cathode catalyst layer temperature is an extreme requirement for *all* cells to reach at least 80 °C before the stack is operated. Coolant circulation is also compared, and, as later shown in

Table 4
Parameter summary, extreme case

Parameter	Value
T_{amb}	−20 °C
$T_{threshold}$	
Trigger temperature	80 °C (middle cell cathode catalyst layer temperature vs. coldest cell cathode catalyst layer temperature)
Heat source	500 W in each cell membrane, e.g. as a result of possible temperature excursions from neighboring electrode chemical reactions [8]

the results, can have a significant impact on the overall stack temperature distribution. A summary of the parameters is shown in Table 4.

3.3.2. Results and discussion

The effect on the membrane of a 500 W input is shown in Fig. 10. The temperature difference between the low and high points within the cell is around 11 °C, or about 10 times the difference found in the 50 W cases shown earlier, reflecting the 10-fold heat input.

However, in Fig. 11, in which the impact of the flow being on or off and of trigger temperature is compared, the cell temperature distribution for the middle portion of the cells remains the same. It is the lack of circulation and the (extreme) requirement for the coldest cell to reach 80 °C that result in a catastrophic condition for the stack (namely, 250 °C membrane temperature for no flow).

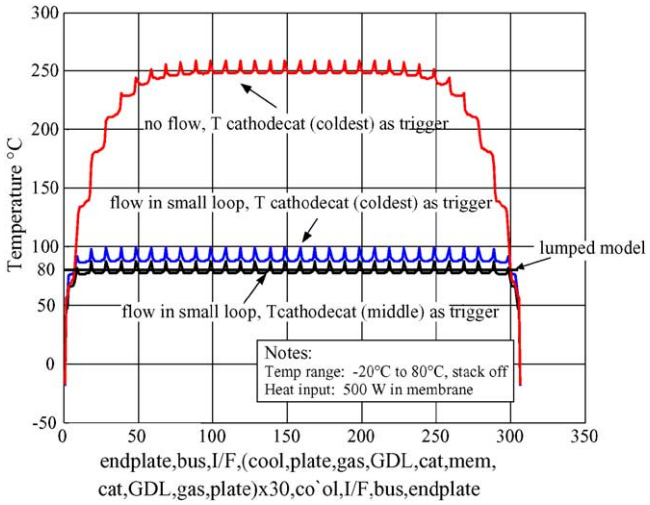

Fig. 11. Stack temperature distribution, extreme case, plot 2.

3.4. Cold start analysis

3.4.1. Simulation conditions and description

In this section, the layered model is used to investigate the advantages and disadvantages of internal heating methods, namely starting the stack alone or after a pre-heat period assisted by other heating methods, and the heat requirements for melting existing ice and/or ice formed from stack reactions. A summary of the parameters is shown in Table 5 and the simulation variations are listed in Table 6.

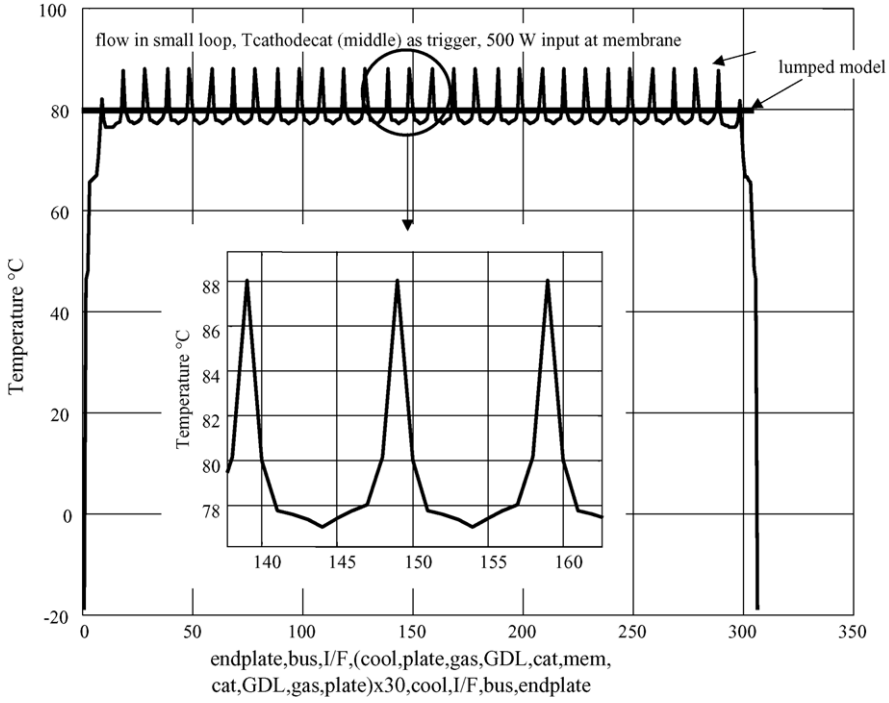

Fig. 10. Stack temperature distribution, extreme case, plot 1.

Table 5
Parameter summary, cold start analysis

Parameter	Value
T_{amb}	−20 °C
$T_{setpoint}$	80 °C
Trigger temperature	Coldest cell cathode catalyst temperature
Heat source output	Internal heat input of 50 W per cell in membrane (e.g. power from electric wire [8])
Flow condition	Small loop (with non-operating external heat source)

Table 6
Simulation variation matrix, cold start analysis

Parameter	Variation
$T_{threshold}$	−20, 0, 20 °C

3.4.2. Results and discussion

3.4.2.1. Heating method comparisons. Fig. 12 shows the time elapsed and energy consumed for the parameters and conditions described in Tables 5 and 6. The bars are divided based on the temperature at which the coldest cell cathode catalyst layer temperature reaches $T_{threshold}$ and the stack begins to operate:

(1) −20 °C, as shown in bar 1,
(2) 0 °C, as shown in bar 2, and
(3) 20 °C, as shown in bar 3.

When the stack begins operation at −20 °C (bar 1), no additional internal heat assists in the warmup process to $T_{setpoint}$ of 80 °C—the heat generated by the stack reactions is the sole source. However, for the other cases, internal heat of 50 W per membrane is used from T_{amb} of −20 °C up to the $T_{threshold}$ (light-colored part of bars) at which the stack begins operation as indicated in the figures (dark-colored part of bars).

The baseline loop configuration used for bars 1–3 is the small loop which includes the thermal mass of a non-operating external heat source.

Note that the total energy consumed is a sum of two parts, separated by the light- and dark-colored parts of the bar chart: (1) the 100% efficient and constant internal heating power plus additional external heating power (if applicable) over time and (2) the H_2 energy consumed by the stack for which efficiency *as a heat source* changes over temperature and time.

When comparing bars 1–3, it is shown that starting stack operation at 0 and 20 °C instead of −20 °C results in a 4% reduction and 2% increase in overall time and a 7% and 14% reduction in overall energy, respectively.

3.4.2.2. Ice formation. Taking the case shown in bar 1 of Fig. 12, in which the stack starts operation at minus 20 °C, one can observe the impact of ice formation on startup characteristics. There are two assumptions that need to be reiterated: (1) the coldest cathode catalyst temperature is used in determining the ice formation and is applied to all cells, even though less ice may form in cells that warm up more quickly, thereby making this assumption a worst case (but "fail safe"), and (2) the impact of ice formation is limited to the thermal characteristics which result from cell current and voltage data for sub-freezing conditions found in the literature [8]. No analysis is made in this paper of the impact of ice on gas diffusion to the catalyst layer.

Fig. 13 shows the formation and melting of ice from product water, and from a combination of product water and ice

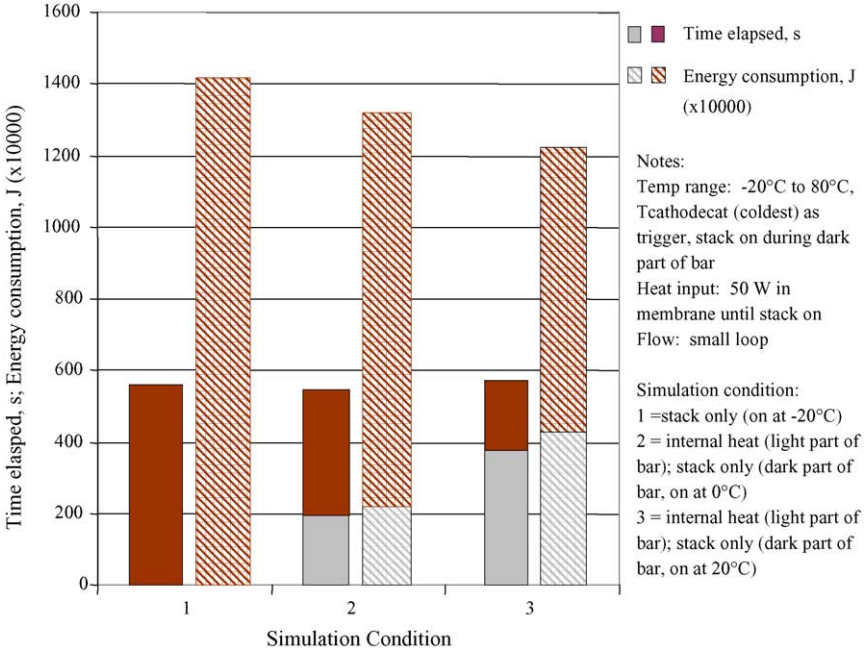

Fig. 12. Time elapsed and energy consumed, cold start analysis.

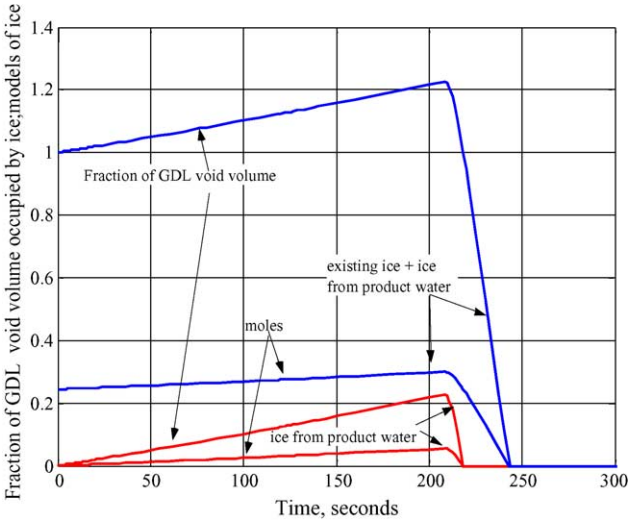

Fig. 13. Moles of ice formed and melted, fraction of GDL void volume occupied.

that may exist from residual water after shutdown. The scenario in which there is existing ice plus ice from product water yields a fraction of the GDL void volume above 1; this is showing that the existing ice completely fills the void volume and product water freezes as an additional layer. The time when melting begins corresponds to the time when the coldest cathode catalyst layer reaches 0 °C as shown in Fig. 14.

Fig. 14 shows the corresponding power required to melt the ice and the effect on the coldest cathode catalyst temperature rise. As shown in the figure, the temperature ceases to rise for the period in which the power is required for melting and then resumes its upward trajectory. As the cell voltage and current characteristics are switched from one set of data in the literature to another based on the temperature ranges within which each was valid, the temperature rise occurs at a different slope at around 25 °C.

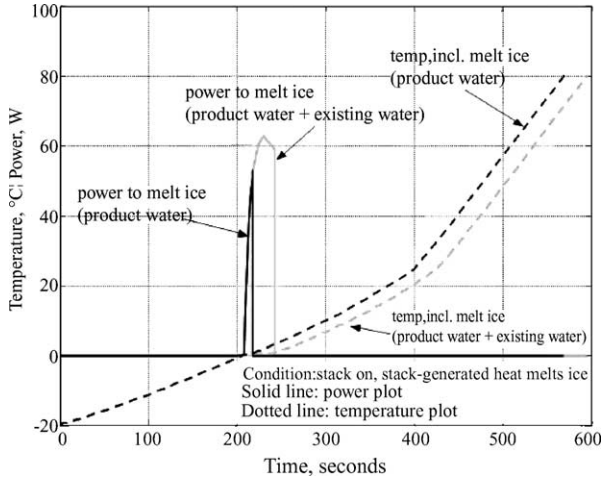

Fig. 14. Temperature and power vs. time, effect of melting ice.

In this section, results were presented using the layered cell cold start thermal model to evaluate various aspects of sub-freezing startup: the advantages and disadvantages of internal heating methods, namely starting the stack alone or after a pre-heat period assisted by other heating methods, and the power requirements for melting ice.

4. Conclusions and recommendations

Four sets of results for a cold start model were presented in this paper: (1) a preliminary lumped analysis, (2) an analysis showing scenarios in which some cell layers or entire cells of the stack were colder than expected as compared to a single lumped parameter temperature of 0 °C, depending on the temperature used in the layered model as the metric for the stack thermal control, (3) an analysis showing scenarios in which some cell layers or entire cells of the stack were hotter than expected as compared to a single lumped parameter temperature of 80 °C, and (4) an evaluation of heating methods together with the impact of ice formation and melting during a sub-freezing startup operation.

Based on the results of the model, several recommendations can be made on the best strategies for startup:

(1) *Use internal stack heating other than stack reactions*. Starting stack operation below 0 °C consumes more time and energy than starting the stack above 0 °C due to ice formation and low heat generation at low temperatures. Even though at low temperatures the stack runs inefficiently and generates more heat than electricity, the amount of heat is insufficient to quickly warm up the stack. Therefore, it is recommended to utilize alternate internal stack heating methods up to 0 °C or above. Such methods, as described in the paper, could include using a resistance wire laminated in the cell membrane or chemical reactions at the electrodes.

(2) *Circulate coolant during warmup*. The warming of the cells by the endplates lags the cells in the middle due to the heat draw by the endplate thermal mass. Circulating coolant ensures that the heat is distributed uniformly throughout the stack.

(3) *Minimize thermal mass that is to be heated*. Even while it is recommended to circulate coolant, the thermal mass of the loop in which the coolant circulates should be minimized to ensure quick warmup of the stack.

(4) *Heat the endplates*. Heating the endplates can mitigate the endplate thermal mass effect on the end cells and quickly bring the end cells to above 0 °C, for example, to prevent ice formation when operating the stack.

(5) *Use a metal-based material for the bipolar plates*. Using stainless steel, for example, can increase the thermal conductivity and reduce the thickness and therefore the thermal mass of the bipolar plates, reducing time and energy consumption during warmup.

Acknowledgements

The authors would like to acknowledge Myron Hoffman and Harry Dwyer of the UC Davis Mechanical and Aeronautical Engineering Department and Daniel Sperling of the UC Davis Institute of Transportation Studies for their contributions to this research.

References

[1] U.S. Department of Energy, Fuel Cell for Transportation, Annual Progress Report, Washington, DC, 2001 (introduction).
[2] U.S. Department of Energy, Progress Report for Hydrogen, Fuel Cells, and Infrastructure Technologies Program, 2002 (Appendix A).
[3] D.J. Friedman, SAE Paper No. 1999-01-0530.
[4] M. Nadal, F. Barbir, Int. J. Hydrogen Energy 21 (1996) 497–505.
[5] P. Atwood, S. Gurski, D.J. Nelson, K.B. Wipke, SAE Paper No. 2001-01-0236.
[6] K. Rajashekara, SAE Paper No. 2000-01-0369.
[7] G. Paganelli, Y. Guezennec, G. Rizzoni, SAE Paper No. 2002-01-0102.
[8] M. Sundaresan, A thermal model to evaluate sub-freezing startup for a direct hydrogen hybrid fuel cell vehicle polymer electrolyte fuel cell stack and system, Dissertation, University of California, Davis, 2004, pp. 6–16.
[9] S. Thomas, M. Zalbowitz, Fuel Cells—Green Power, U.S. DOE, Los Alamos, 1999, p. 5.
[10] G. Maggio, V. Recupero, C. Mantegazza, J. Power Sources 62 (1996) 167–174.
[11] Y. Zhang, M. Ouyang, Q. Lu, J. Luo, X. Li, Appl. Therm. Eng. 24 (2004) 501–513.
[12] J. Wind, A. LaCroix, S. Braeuninger, P. Hedrich, C. Heller, M. Schudy, in: W. Vielstich, A. Lamm, H. Gasteiger (Eds.), Handbook of Fuel Cells—Fundamentals, Technology and Applications, vol. 3: Fuel Cell Technology and Applications, John Wiley & Sons Ltd., Chichester, 2003.